Multi-microscopy Characterisation of III-nitride Devices and Materials

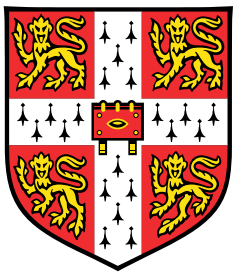

Christopher Xiang Ren

Department of Materials Science and Metallurgy
University of Cambridge

This dissertation is submitted for the degree of
Doctor of Philosophy

Wolfson College

April 2016

I would like to dedicate this thesis to my loving parents ...

Declaration

I hereby declare that except where specific reference is made to the work of others, the contents of this dissertation are original and have not been submitted in whole or in part for consideration for any other degree or qualification in this, or any other university. This dissertation is my own work and contains nothing which is the outcome of work done in collaboration with others, except as specified in the text and Acknowledgements. This dissertation contains fewer than 65,000 words including appendices, bibliography, footnotes, tables and equations and has fewer than 150 figures.

Christopher Xiang Ren
April 2016

Acknowledgements

And I would like to acknowledge ...

Abstract

This is where you write your abstract ...

Table of contents

List of figures

List of tables

Nomenclature

Acronyms / Abbreviations

1-D	One-Dimensional
AlN	Aluminium Nitride
EL	Electroluminescence
ET	Electron Tomography
FIBT	Focussed Ion Beam Tomography
GaAs	Gallium Arsenide
GaN	Gallium Nitride
InN	Indium Nitride
LED	Light-Emitting Diode
SPS	Single Photon Source

Nomenclature

Acronyms / Abbreviations

1-D	One-Dimensional
AlN	Aluminium Nitride
EL	Electroluminescence
ET	Electron Tomography
FIBT	Focussed Ion Beam Tomography
GaAs	Gallium Arsenide
GaN	Gallium Nitride
InN	Indium Nitride
LED	Light-Emitting Diode
SPS	Single Photon Source

Chapter 1

Introduction

Gallium nitride (GaN) has been termed the 'most important semiconductor material since silicon' [1], and indeed the influence of this incredible material and it's associated alloys (termed III-nitrides) is pervasive in modern society. The impact of III-nitride materials is perhaps best evidenced by the global transition from traditional lighting sources to semiconductor lighting solutions based on III-nitride materials. Since the first demonstration of a high-brightness blue light emitting diode (LED) in 1991 by Shuji Nakamura [2], the widespread use of LEDs for general lighting purposes has blossomed into a multi-billion pound industry. The extraordinary optical properties of III-nitride materials have enabled their application outside of the lighting industry: the development of III-nitride based lasers has found applications in telecommunications [3], medicine [4] and data storage . Furthermore, III-nitride optical emitters have been used as single photon sources (SPSs) which have applications in cryptography for secure communications [5].

The optoelectronic properties of III-nitride materials are somewhat astonishing: GaN suffers from a defect density several orders of magnitude higher than other optically active semiconductor materials such as gallium arsenide (GaAs) [6] yet is still optically active. Despite this, the effects of defects originating from the heteropitaxial growth of GaN are clearly deleterious when considering III-nitride device operation. This work aims to explore the manner in which the microstructural properties of photonic III-nitride devices affect their performance by combining multiple microscopy techniques, an approach we term 'multi-microscopy', thus allowing us to link specific structural features with emissive properties at the device level. The experimental research in this thesis is separated into four main sections.

The first section details the investigation of inhomogeneous electroluminescence (EL) of indium gallium nitride (InGaN) quantum well (QW) LEDs. By employing the use of scanning probe techniques, electron microscopy and spectroscopy the underpinning cause of LED behaviour was elucidated and reported.

The second section involves microscopy-based investigation into the mechanisms behind incomplete etching in the fabrication of III-nitride based microdisk cavities and the effect of this issue on the overall optical performance of these cavities
The third section describes the microscopy of one dimensional (1-D) photonic crystal cavity (PCC) 'nanobeam' cavities. The intrinsic resistance of III-nitride based materials can often result in improperly etched features, which can results in high optical losses in cavities. This section concerns the use of tomographic techniques such as electron tomography (ET) and focussed ion beam tomography (FIB-T) to investigate the effect of these issues on the emission of III-nitride nanobeam cavities.

1.1 III-Nitride Material Properties

1.1.1 Crystal Structure

GaN can crystallise into two distinct crystal structures: hexagonal (wurtzite) and cubic (zinc blende and rock salt). Under ambient conditions, wurtzite GaN is the most commonly studied form as it is the most structurally stable. Thus, the work discussed in this thesis concerns wurtzite III-nitrides. A schematic of a wurtzite III-nitride crystal structure is shown in Fig.**??** and consists of stacked hexagonal close-packed planes following an ABABAB stacking sequence. Atoms of the respective elements are tetrahedrally bonded to one another. However, in the case of III-nitrides this structure deviates from ideal tetrahedral bonding and results in a non-zero dipole moment for each unit cell which will be discussed in the following sections.
A 4-index Miller-Bravais notation (hkil) is used to denote the crystal planes where the index i is defined by the relation:

$$i = -(h+k) \tag{1.1}$$

The crystallographic planes (0001), (1-100) and (11-20) shown in Fig.**??** are often termed the c, m and a-planes in the literature. The fundamental unit cell of the wurtzite GaN crystal structure and its associated lattice parameters **a** and **c** is shown in Fig.1.1

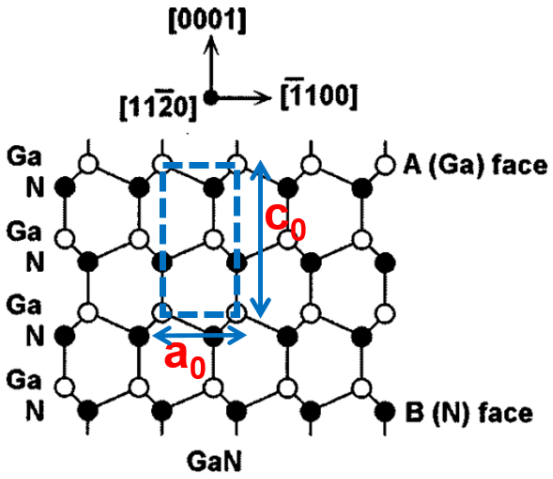

Fig. 1.1 Unit cell (dashed line) for GaN crystal structure and lattice parameters $\mathbf{a_0}, \mathbf{c_0}$. Adapted from [7]

Other members of the III-nitride materials such as indium nitride (InN) or aluminium nitride (AlN) have different lattice parameters due to the differing atomic radii of aluminium and indium relative to gallium.

Alloy	**a** (Å) at T = 300K	**c** (Å) at T = 300K
GaN	3.189	5.185
InN	3.545	5.703
AlN	3.112	4.982

Table 1.1 Room temperature lattice parameters for GaN, InN and AlN [8].

III-nitride photonic devices are often heterostructures consisting of ternary alloys the materials shown in Table **??**. Lattice parameters of a relaxed ternary alloy $A_xB_{1-x}N$ can be estimated using Vegard's law [9]:

$$\mathbf{a} = x\mathbf{a}_{AN} + (1-x)\mathbf{a}_{BN} \tag{1.2}$$

$$\mathbf{c} = x\mathbf{c}_{AN} + (1-x)\mathbf{c}_{BN} \tag{1.3}$$

Typical indium compositions for blue LEDs range between 15-20 %, which leads to a considerable lattice mismatch of approximately 2 %, resulting in considerable amounts of strain in these GaN/InGaN heterostructures.

1.1.2 Band Structure

One of the principal driving factors behind the interest in III-nitrides for photonic devices is their direct bandgap which collectively spans the visible spectrum and beyond. The bandgap of III-nitride binary alloys is given below in Table.1.2.

Alloy	Bandgap (eV)
GaN	3.51
InN	0.78
AlN	6.25

Table 1.2 Direct bandgaps of GaN, InN and AlN [8].

Ternary alloying modifies the bandgap as shown in Fig.1.2. In theory the entire range of 0.78-6.25 eV is accessible through alloying, though material limitations reduce the full effective range for III-nitride devices [10].

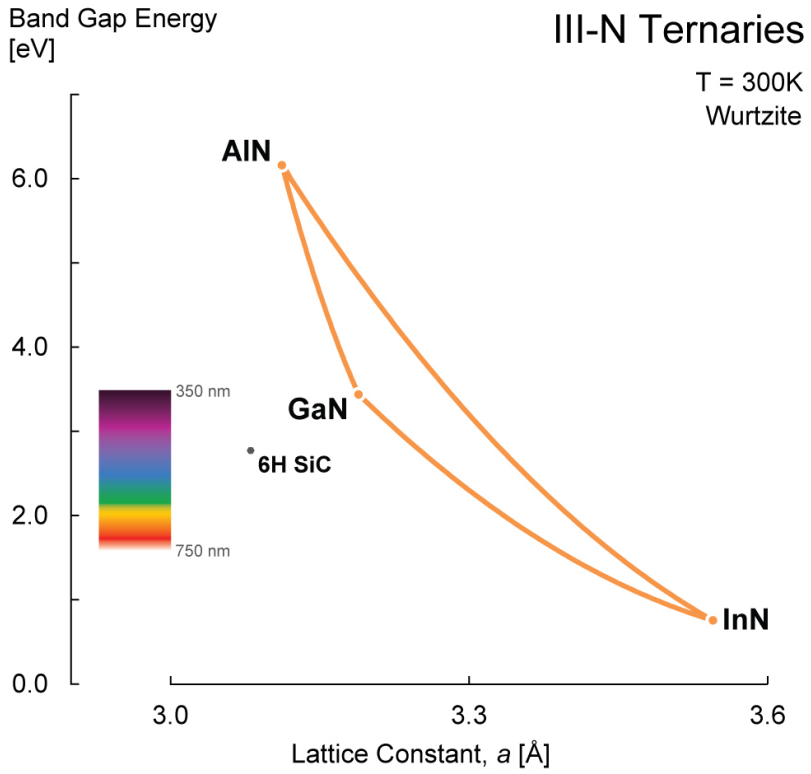

Fig. 1.2 Bandgap at room temperature for III-nitride materials with the visible spectrum shown on the left. Courtesy of K. Montgomery.

The bandgap of a ternary alloy $A_xB_{1-x}N$ is given by a modified Vegard's Law:

$$E_g = xE_g^{AN} + (1-x)E_g^{BN} - x(1-x)C \tag{1.4}$$

Where C is a bowing parameter which accounts for deviation from a linear relation between ternary alloy composition and bandgap energy. The value of the InGaN bowing parameter has been widely debated in the literature due to the lack of a reliable value for the bandgap energy for InN [8]. Although the current value of 1.4 eV is reported, there are also suggestions the bowing parameter may be composition dependent [11–13].
In considering the optical properties of III-nitride materials it is also important to consider the effects of impurities and defects. Crystal disorder introduces further energy states which would be 'forbidden' in an ideal crystal lattice leading to an effective 'smearing' of the bandgap. Sub-bandgap absorption can occur due to the introduction of these defective states. The smearing out of the absorption edge of the material is known as the 'Urbach tail', and can be a highly deleterious source of loss in III-nitride cavity structures [14].

Quantum Confinement Effects

The first prototype high-brightness blue III-nitride LED consisted of a GaN *p-n* junction, or a 'homojunction' [2], however modern LED structures consist of heterostructures known as quantum wells. QWs consist of a thin layer of low bandgap material between two quantum barriers with a higher bandgap. Carriers in the low bandgap material are effectively confined in one direction, hence the term 'quantum well'. This confinement leads to the discretisation of the carrier wavefunctions within the well, as shown schematically in Fig.1.3.

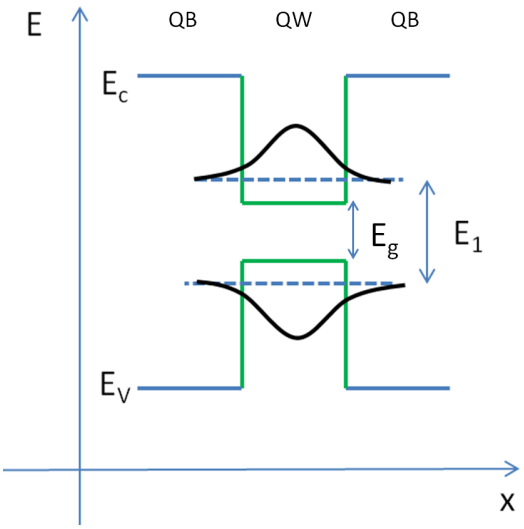

Fig. 1.3 Band diagram of a quantum well. The bandgap of the well material is denoted E_g, the energy of the ground state transition is denoted E_1 and the conduction and valence bands are denoted E_c, E_v respectively [16].

Thus the energy of the transition in the QW is given by the following relation:

$$h\nu = E_1 - E_{ex} \tag{1.5}$$

where E_1 is the energy of the ground state transition and E_{ex} is the exciton binding energy. For an infinite potential well of thickness L, the ground state E_1 is given by:

$$E_1 = \frac{\hbar^2 \pi_2}{2m^* L^2} \tag{1.6}$$

where $\hbar$ is the reduced Plank constant, m^* is the carrier effective mass. As such, the energy of the optical transition can be related to the thickness of the well.

1.1.3 Built-in Fields

III-nitride materials in wurtzite structure are termed 'polar' materials, due to the fact they exhibit a spontaneous polarisation field [15]. This occurs due to III-nitride bonding structure deviating from an ideal tetrahedral structure along the (0001) axis along the crystal, combined with the ionicity of the bond [16]. This deviation causes each unit cell to possess a non-zero dipole moment along the principal axis of the tetrahedral bonding structure, resulting in an overall spontaneous polarization in the crystal. As the III-nitride wurtzite structure is non-centrosymmetric, the direction of the polarization depends on whether the crystal exhibits (+ c) or (-c) polarity, as shown in Fig.1.4

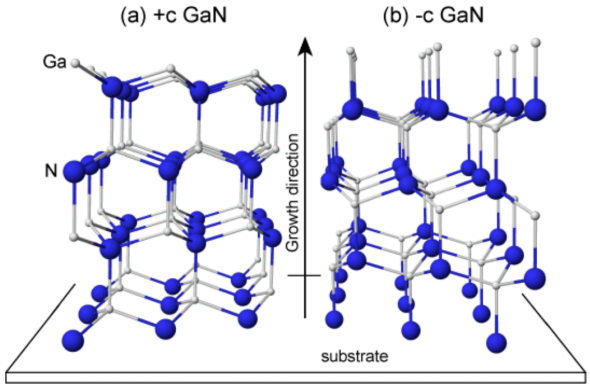

Fig. 1.4 Illustration of Ga-face (+ *c*) and N-face (-*c*) GaN wrutzite crystal exhibiting polarity along the *c*-axis [17].

This non-zero dipole moment is particularly strong for III-nitrides relative to other III-V semiconductors due to the strong electronegativity and small size of nitrogen compared to other group V elements, resulting in a metal-nitrogen bond with greater ionicity than other III-V bonds [18]. Fig.1.5 shows a GaN unit cell with lattice parameters *c* and *a* denoted.

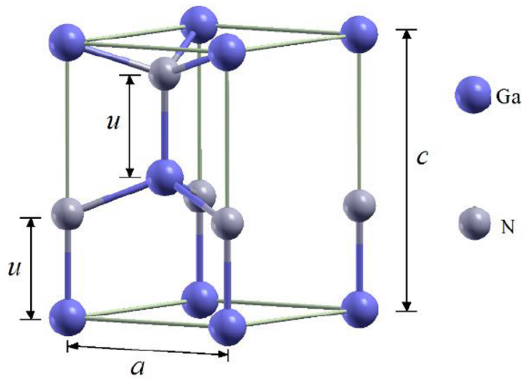

Figure 1. Unit cell 1x1-MN/GaN (M = V, Cr and Mn) multilayers.

Fig. 1.5 GaN unit cell with lattice parameters *c* and *a* [19]

If all nearest neighbour bond lengths are equal, an ideal hexagonal closed packed crystal exhibiting zero spontaneous polarisation would have a ratio of lattice parameters denoted by:

$$\frac{c}{a} = (\frac{8}{3})^{0.5} = 1.63299 \tag{1.7}$$

The degree of spontaneous polarisation observed in III-nitride materials is thus determined by the amount their lattice parameter ratio deviates from this ideal value. The values for bulk III-nitride materials are given in Table.1.3.

Alloy	$\frac{c}{a}$
GaN	1.6259
InN	1.6116
AlN	1.6010

Table 1.3 Bulk $\frac{c}{a}$ ratios for GaN, InN and AlN [16].

A lower $\frac{c}{a}$ ratio indicates a higher angle between the three bonds at the base of the tetrahedral bonding structure, resulting in a lower compensation polarisation along the (0001) axis and a higher spontaneous polarisation. Thus according to Table.1.2 the strongest spontaneous polarisation is observed in AlN and the weakest in GaN.
It is important to note that materials which exhibit spontaneous polarisation also exhibit piezoelectric polarisation [15]. Strain experienced by the material results in the distortion in of the crystal lattice, which can either alleviate or exacerbate the deviation from the ideal tetrahedral structure resulting in an additional polarisation. This piezoelectric polarization is a crucial consideration in III-nitride devices which often consist of QW heterostructures: lattice mismatches with underlying layers result in the expansion or contraction of III-nitride films. Interestingly two different polarisation configurations are obtained for AlGaN and InGaN coherently strained to GaN. In the case of InGaN the piezoelectric field acts against the spontaneous field, whilst the opposite is true for AlGaN strained to GaN. Within the context of visible light LEDs, InGaN containing QWs are dominated by the piezoelectric contribution to the polarization fields [20] due to the sizeable lattice mismatch between GaN and InN (11%) [21].

The Quantum Confined Stark Effect

As previously discussed, III-nitride photonic devices often make use of heterostructures known as quantum wells, which enhance radiative efficiency by confining carrier wavefunctions over a range of several nanometres. Given the presence of built-in fields in III-nitride materials, it is important to consider the effect polarisation fields will have on the band structure and thus optical properties of quantum wells as shown in Fig.1.6

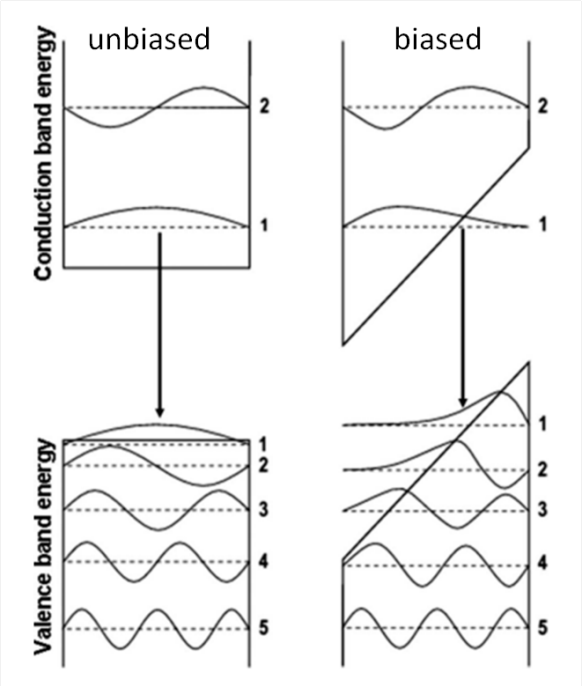

Fig. 1.6 Unbiased and biased quantum well energy levels with associated carrier wavefunctions. Under an applied field the overlap between the electron and hole carrier wavefunctions is reduced [22].

The transition from a rectangular to a 'sawtooth'-shaped potential well results in the reduction in energy of the optical transition, meaning the photons emitted from the QW are red-shifted. However, as the carrier density within the QW is increased, by either optical or electrical injection, the polarization fields are effectively screened resulting in a carrier density-dependent optical transition energy.
A further effect of the polarization fields is to spatially separate the carrier wave functions, thus reducing their overlap as shown in Fig.1.6. This results in a reduced probability for the radiative recombination carriers thus reducing the efficiency of III-nitride QW emitters.

1.1.4 Defects in III-nitrides

Many issues with III-nitride based optoelectronic devices arise from the high defect densities present. Dislocation densities tend to be several orders of magnitude higher for nitride devices relative to other III-V materials due to the lack of a low cost, widely-available lattice matched substrate [6]. Lattice mismatch and alloy-dependent growth temperatures results in the presence of imperfections in the crystal structure of the epitaxial film known as defects. These defects can result in perturbations to the electrical and optical properties of an 'ideal' crystal, and are often classified based on their spatial dimensions. 0-D defects are often

referred to as point defects, 1-D defects are commonly termed linear defects or dislocations, 2-D defects are known as planar defects or stacking faults, and there are a variety of 3-D defects known as volume defects.

0-D Defects

Point defects exist in four main forms, shown in Fig.1.7. Vacancies, where an atom is missing from the lattice, and self-interstitial point defects are termed 'native defects': there is no inclusion of foreign atoms. These two types of intrinsic point defects are shown in Fig.1.7 a) and b) respectively.
In the case of GaN, three types of vacancies can exist: gallium vacancies, nitrogen vacancies and divacancies. The gallium vacancy (V_{Ga}) which has a low formation energy in *n*-type GaN and is acceptor-like, this vacancy has a low migration barrier. Due to this low migration energy, it is expected that gallium vacancies form complexes with more stable defects. Gallium vacancies and associated complexes are thought to be the cause of yellow luminescence observed in *n*-type GaN. Nitrogen vacancies initially attracted a large amount of interest due to the common belief that their energy levels were close to or within the conduction band. Due to this, the *n*-type conductivity of undoped GaN was attributed to nitrogen vacancies. However, calculations have shown the thermal equilibrium of nitrogen vacancies to be too low to account for the observed conductivity. Nitrogen vacancies are also expected to have relatively low migration barriers, indicating complexes involving more stable defects may occur during high-temperature growth or annealing, especially in *p*-type GaN [23]. Divacancies have high formation energy in GaN and are not expected to form in large concentrations [23].
The inclusion of foreign atoms can result in a foreign interstitial point defect, or a substitional impurity, both are shown in Fig.1.7 c) and d) respectively. The formation of self-interstitial or antisite (swapping of Ga and N lattice positions in the lattice) have a low occurence due to the small lattice constant of GaN and large size mismatch between Ga and N atoms [23].

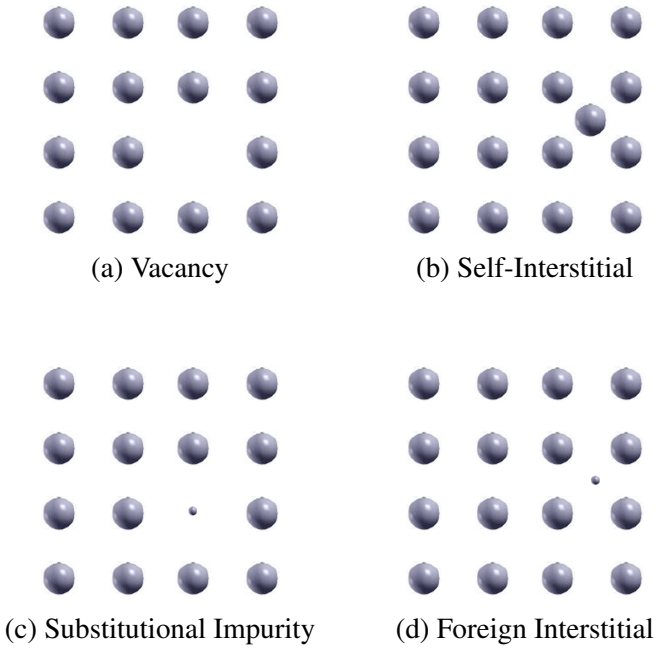

(a) Vacancy (b) Self-Interstitial

(c) Substitutional Impurity (d) Foreign Interstitial

Fig. 1.7 Point Defects: a) vacancy, b) self-intertitial, c) substitutional impurity and d) foreign interstitial.

Point defects are responsible for a plethora of deleterious effects at the device level in III-nitrides: they can reduce radiative efficiency, produce undesired luminescence act and as parasitic current paths [23].

1-D Defects

Dislocations in GaN epilayers can be divided into two main categories, misfitdislocations (MDs) and threading dislocations (TDs). Misfit dislocations occurthrough the release of misfit strain at interfaces between two crystals of differing lattice constants. The process is shown in Fig.1.7 below and can be described as such: a film with a lattice parameter greater than the substrate is grown, which is typical for GaN epilayers (GaN on sapphire or InGaN on GaN) and as a result the grown layer experiences compressive stress to form what is known as a pseudomorphic layer. In effect, the top layer is strained (as it has a smaller lattice parameter) and matched to the lower layer. As the top film reaches a critical thickness, the pseudomorphic relationship is broken, and strain relaxation occurs through the formation of MDs.

1.2 III-nitride Cavities

1.2.1 Cavity characteristics

1.2.2 Cavity Designs

Chapter 2

Experimental Methods

2.1 Atomic Force Microscopy

2.2 Hyperspectral Electroluminescence Mapping

2.3 Scanning Electron Microscopy and Cathodoluminescence

2.4 Photoluminescence

2.5 Dual Beam Scanning Electron microscopy with a Focussed Ion Beam

2.5.1 Fabrication

2.5.2 Tomography

2.6 Transmisson Electron Microscopy

2.6.1 Tomography

2.7 Hidden section

Lorem ipsum dolor sit amet, *consectetur adipiscing elit*. In magna nisi, aliquam id blandit id, congue ac est. Fusce porta consequat leo. Proin feugiat at felis vel consectetur. Ut

tempus ipsum sit amet congue posuere. Nulla varius rutrum quam. Donec sed purus luctus, faucibus velit id, ultrices sapien. Cras diam purus, tincidunt eget tristique ut, egestas quis nulla. Curabitur vel iaculis lectus. Nunc nulla urna, ultrices et eleifend in, accumsan ut erat. In ut ante leo. Aenean a lacinia nisl, sit amet ullamcorper dolor. Maecenas blandit, tortor ut scelerisque congue, velit diam volutpat metus, sed vestibulum eros justo ut nulla. Etiam nec ipsum non enim luctus porta in in massa. Cras arcu urna, malesuada ut tellus ut, pellentesque mollis risus.Morbi vel tortor imperdiet arcu auctor mattis sit amet eu nisi. Nulla gravida urna vel nisl egestas varius. Aliquam posuere ante quis malesuada dignissim. Mauris ultrices tristique eros, a dignissim nisl iaculis nec. Praesent dapibus tincidunt mauris nec tempor. Curabitur et consequat nisi. Quisque viverra egestas risus, ut sodales enim blandit at. Mauris quis odio nulla. Cras euismod turpis magna, in facilisis diam congue non. Mauris faucibus nisl a orci dictum, et tempus mi cursus.

Etiam elementum tristique lacus, sit amet eleifend nibh eleifend sed [1]. Maecenas dapibu augue ut urna malesuada, non tempor nibh mollis. Donec sed sem sollicitudin, convallis velit aliquam, tincidunt diam. In eu venenatis lorem. Aliquam non augue porttitor tellus faucibus porta et nec ante. Proin sodales, libero vitae commodo sodales, dolor nisi cursus magna, non tincidunt ipsum nibh eget purus. Nam rutrum tincidunt arcu, tincidunt vulputate mi sagittis id. Proin et nisi nec orci tincidunt auctor et porta elit. Praesent eu dolor ac magna cursus euismod. Integer non dictum nunc.

[1] My footnote goes blah blah blah! ...

Subplots

I can cite Wall-E (see Fig. 3.1b) and Minions in despicable me (Fig. 3.1c) or I can cite the whole figure as Fig. 3.1

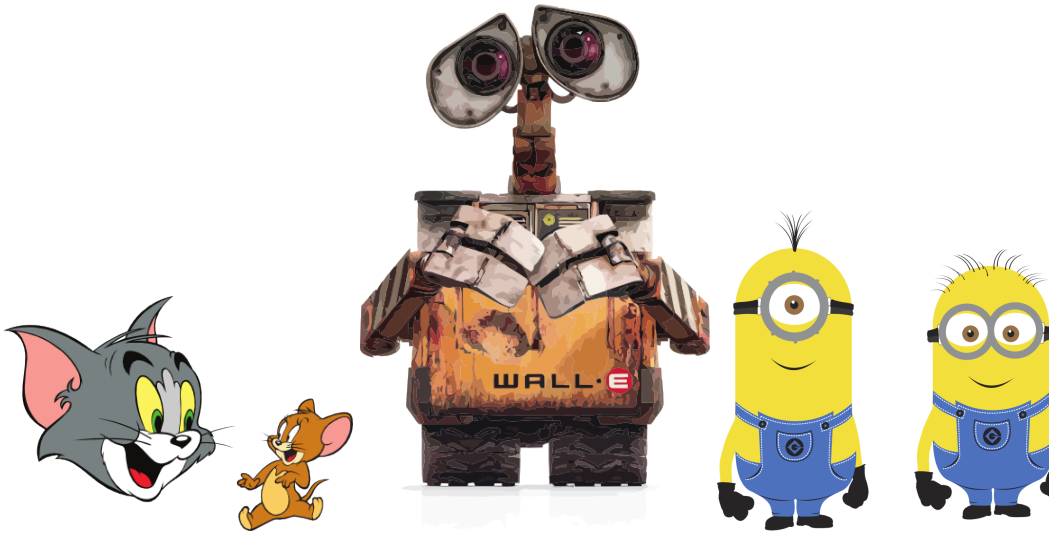

(a) Tom and Jerry (b) Wall-E (c) Minions

Fig. 2.1 Best Animations

Chapter 3

Inhomogeneous Electroluminescence in InGaN QW LEDs

3.1 Background

$In_xGa_{1-x}N$/GaN quantum well (QW) structures are key structures in present day light emitting diodes in the visible wavelengths. Despite the growth of III-nitride LEDs into a gigantic market with a projected overall worth of 64 billion EUR by 2020, III-nitride alloys suffer from a plethora of material issues arising from heteroepitaxial growth on foreign substrates with large lattice mismatches [6]. A notorious issue in III-nitride growth is the high density of threading dislocations which are the source of highly undesirable effects in diode structures such as non-radiative recombination [24] and leakage current [6].
Threading dislocations have been shown to result in inverted pyramidal defects at the surface of nitride epilayers, known as 'V defects'. The effect of these defects on LED performance is hotly debated in literature as they are expected by many to hinder LED performance due to their association with TDs. However, it has been shown that narrower QWs along the sidewalls of V-defects serve to screen carriers from the non-radiative centres at TDs

Enumeration

1. The first topic is dull
2. The second topic is duller
    (a) The first subtopic is silly
    (b) The second subtopic is stupid

3. The third topic is the dullest

itemize

- The first topic is dull
- The second topic is duller
  - The first subtopic is silly
  - The second subtopic is stupid
- The third topic is the dullest

description

The first topic is dull

The second topic is duller

The first subtopic is silly

The second subtopic is stupid

The third topic is the dullest

3.2 Hidden section

Lorem ipsum dolor sit amet, *consectetur adipiscing elit*. In magna nisi, aliquam id blandit id, congue ac est. Fusce porta consequat leo. Proin feugiat at felis vel consectetur. Ut tempus ipsum sit amet congue posuere. Nulla varius rutrum quam. Donec sed purus luctus, faucibus velit id, ultrices sapien. Cras diam purus, tincidunt eget tristique ut, egestas quis nulla. Curabitur vel iaculis lectus. Nunc nulla urna, ultrices et eleifend in, accumsan ut erat. In ut ante leo. Aenean a lacinia nisl, sit amet ullamcorper dolor. Maecenas blandit, tortor ut scelerisque congue, velit diam volutpat metus, sed vestibulum eros justo ut nulla. Etiam nec ipsum non enim luctus porta in in massa. Cras arcu urna, malesuada ut tellus ut, pellentesque mollis risus.Morbi vel tortor imperdiet arcu auctor mattis sit amet eu nisi. Nulla gravida urna vel nisl egestas varius. Aliquam posuere ante quis malesuada dignissim. Mauris ultrices tristique eros, a dignissim nisl iaculis nec. Praesent dapibus tincidunt mauris nec tempor. Curabitur et consequat nisi. Quisque viverra egestas risus, ut sodales enim blandit at. Mauris quis odio nulla. Cras euismod turpis magna, in facilisis diam congue non. Mauris faucibus nisl a orci dictum, et tempus mi cursus.

Etiam elementum tristique lacus, sit amet eleifend nibh eleifend sed [1]. Maecenas dapibu augue ut urna malesuada, non tempor nibh mollis. Donec sed sem sollicitudin, convallis velit aliquam, tincidunt diam. In eu venenatis lorem. Aliquam non augue porttitor tellus faucibus porta et nec ante. Proin sodales, libero vitae commodo sodales, dolor nisi cursus magna, non tincidunt ipsum nibh eget purus. Nam rutrum tincidunt arcu, tincidunt vulputate mi sagittis id. Proin et nisi nec orci tincidunt auctor et porta elit. Praesent eu dolor ac magna cursus euismod. Integer non dictum nunc.

[1] My footnote goes blah blah blah! ...

Subplots

I can cite Wall-E (see Fig. 3.1b) and Minions in despicable me (Fig. 3.1c) or I can cite the whole figure as Fig. 3.1

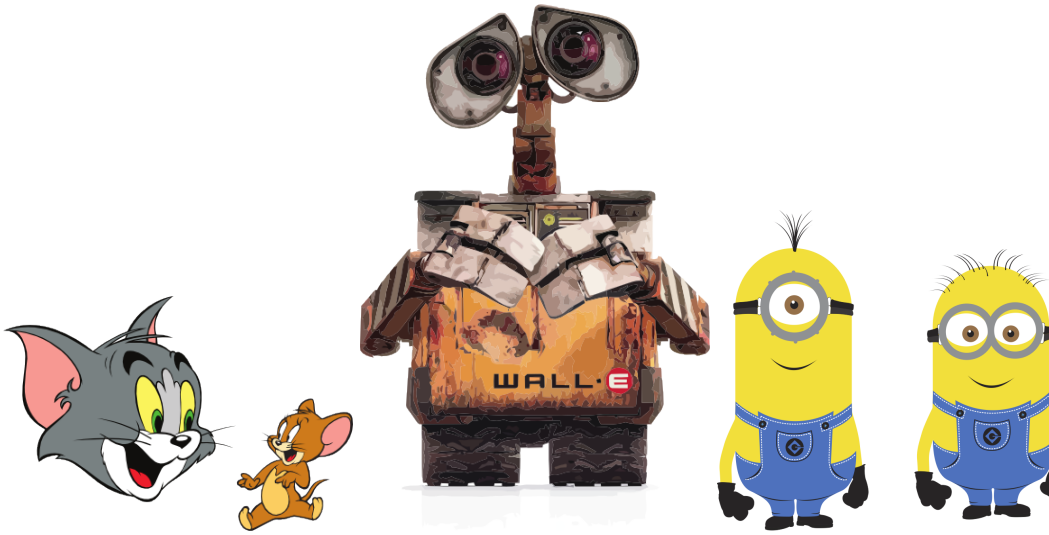

(a) Tom and Jerry (b) Wall-E (c) Minions

Fig. 3.1 Best Animations

References

[1] C. J. Humphreys, "USE Solid-State Lighting," *MRS Bulletin*, vol. 33, no. April, pp. 459–471, 2008.

[2] S. Nakamura, T. Mukai, and M. Senoh, "High-Power GaN P-N Junction Blue-Light-Emitting Diodes," *Japanese Journal of Applied Physics*, vol. 30, no. 12A, pp. 1998–2001, 1991.

[3] S. Najda, P. Perlin, L. Marona, M. Leszczy, R. Czernecki, S. Watson, A. E. Kelly, A. Malcolm, P. Blanchard, and H. White, "Novel laser diode technology for free-space communications," *SPIE*, pp. 10–12, 2015.

[4] H. Berlien, H. Breuer, G. Müller, N. Krasner, T. Okunata, and D. Sliney, *Applied Laser Medicine*. Springer Berlin Heidelberg, 2012.

[5] S. Kako, C. Santori, K. Hoshino, S. Götzinger, Y. Yamamoto, and Y. Arakawa, "A gallium nitride single-photon source operating at 200 K.," *Nature materials*, vol. 5, pp. 887–92, nov 2006.

[6] S. E. Bennett, "Dislocations and their reduction in GaN," *Materials Science and Technology*, vol. 26, no. 9, pp. 1017–1028, 2010.

[7] E. T. Yu, X. Z. Dang, P. M. Asbeck, S. S. Lau, and G. J. Sullivan, "Spontaneous and piezoelectric polarization effects in III–V nitride heterostructures," *Journal of Vacuum Science & Technology B: Microelectronics and Nanometer Structures*, vol. 17, p. 1742, 1999.

[8] I. Vurgaftman and J. R. Meyer, "Band parameters for nitrogen-containing semiconductors," *Journal of Applied Physics*, vol. 94, no. 6, pp. 3675–3696, 2003.

[9] M. E. Vickers, M. J. Kappers, T. M. Smeeton, E. J. Thrush, J. S. Barnard, and C. J. Humphreys, "Determination of the indium content and layer thicknesses in InGaN/GaN quantum wells by x-ray scattering," *Journal of Applied Physics*, vol. 94, no. 3, pp. 1565–1574, 2003.

[10] F. Scholz, "Semipolar GaN grown on foreign substrates: a review," *Semiconductor Science and Technology*, vol. 27, p. 024002, feb 2012.

[11] J. Wu, W. Walukiewicz, K. M. Yu, J. W. Ager, E. E. Haller, H. Lu, and W. J. Schaff, "Small band gap bowing in In1-xGaxN alloys," *Applied Physics Letters*, vol. 80, no. 25, pp. 4741–4743, 2002.

[12] M. D. McCluskey, C. G. Van de Walle, L. T. Romano, B. S. Krusor, and N. M. Johnson, "Effect of composition on the band gap of strained InxGa1-xN alloys," *Journal of Applied Physics*, vol. 93, no. 7, pp. 4340–4342, 2003.

[13] P. G. Moses and C. G. Van De Walle, "Band bowing and band alignment in InGaN alloys," *Applied Physics Letters*, vol. 96, no. 2, pp. 2–5, 2010.

[14] T. J. Puchtler, A. Woolf, T. Zhu, D. Gachet, E. L. Hu, and R. a. Oliver, "Effect of Threading Dislocations on the Quality Factor of InGaN/GaN Microdisk Cavities," *ACS Photonics*, vol. 2, pp. 137–143, 2015.

[15] O. Ambacher and J. Majewski, "Pyroelectric properties of Al (In) GaN/GaN hetero-and quantum well structures," *Journal of physics: ...*, vol. 3399, 2002.

[16] C. X. Ren, "Polarisation fields in III-nitrides: effects and control," *Materials Science and Technology*, vol. 00, no. 0, p. 1743284715Y.000, 2015.

[17] M. Sumiya and S. Fuke, "Review of polarity determination and control of GaN," *MRS Internet Journal of Nitride Semiconductor Research*, vol. 9, no. 1, pp. 1–32, 2004.

[18] C. Wood and D. Jena, *Polarization Effects in Semiconductors: From Ab Initio Theory to Device Applications*. Springer, 2007.

[19] J. E. R. Miguel, C. J. Gladys, and O. L. César, "Computational calculation of the electronic and magnetic properties of 1x1-MN / GaN (M = V , Cr and Mn) multilayers," *International Journal of Physical Sciences*, vol. 9, no. 24, pp. 538–544, 2014.

[20] V. Fiorentini, F. Bernardini, F. D. Sala, A. D. Carlo, P. Lugli, and T. Vergata, "Effects of macroscopic polarization in III-V nitride multiple quantum wells," *Physical Review B*, vol. 60, no. 12, pp. 8849–8858, 1999.

[21] S. F. Chichibu, A. Uedono, T. Onuma, B. a. Haskell, A. Chakraborty, T. Koyama, P. T. Fini, S. Keller, S. P. Denbaars, J. S. Speck, U. K. Mishra, S. Nakamura, S. Yamaguchi, S. Kamiyama, H. Amano, I. Akasaki, J. Han, and T. Sota, "Origin of defect-insensitive emission probability in In-containing (Al,In,Ga)N alloy semiconductors.," *Nature materials*, vol. 5, pp. 810–6, oct 2006.

[22] J. H. Ryou, P. D. Yoder, J. Liu, Z. Lochner, H. S. Kim, S. Choi, H. J. Kim, and R. D. Dupuis, "Control of quantum-confined stark effect in InGaN-based quantum wells," *IEEE Journal on Selected Topics in Quantum Electronics*, vol. 15, no. 4, pp. 1080–1091, 2009.

[23] M. A. Reshchikov and H. Morko, "Luminescence properties of defects in GaN," *Journal of Applied Physics*, vol. 97, no. 6, 2005.

[24] M. Albrecht, J. L. Weyher, B. Lucznik, I. Grzegory, and S. Porowski, "Nonradiative recombination at threading dislocations in n-type GaN: Studied by cathodoluminescence and defect selective etching," *Applied Physics Letters*, vol. 92, no. 23, pp. 0–3, 2008.

Appendix A

How to install LaTeX

Windows OS

TeXLive package - full version

1. Download the TeXLive ISO (2.2GB) from
   https://www.tug.org/texlive/
2. Download WinCDEmu (if you don't have a virtual drive) from
   http://wincdemu.sysprogs.org/download/
3. To install Windows CD Emulator follow the instructions at
   http://wincdemu.sysprogs.org/tutorials/install/
4. Right click the iso and mount it using the WinCDEmu as shown in
   http://wincdemu.sysprogs.org/tutorials/mount/
5. Open your virtual drive and run setup.pl

or

Basic MikTeX - TeX distribution

1. Download Basic-MiKTeX(32bit or 64bit) from
   http://miktex.org/download
2. Run the installer
3. To add a new package go to Start » All Programs » MikTex » Maintenance (Admin)
   and choose Package Manager

4. Select or search for packages to install

TexStudio - TeX editor

1. Download TexStudio from
   http://texstudio.sourceforge.net/#downloads

2. Run the installer

Mac OS X

MacTeX - TeX distribution

1. Download the file from
   https://www.tug.org/mactex/

2. Extract and double click to run the installer. It does the entire configuration, sit back and relax.

TexStudio - TeX editor

1. Download TexStudio from
   http://texstudio.sourceforge.net/#downloads

2. Extract and Start

Unix/Linux

TeXLive - TeX distribution

Getting the distribution:

1. TexLive can be downloaded from
   http://www.tug.org/texlive/acquire-netinstall.html.

2. TexLive is provided by most operating system you can use (rpm,apt-get or yum) to get TexLive distributions

Installation

1. Mount the ISO file in the mnt directory

   ```
   mount -t iso9660 -o ro,loop,noauto /your/texlive####.iso /mnt
   ```

2. Install wget on your OS (use rpm, apt-get or yum install)

3. Run the installer script install-tl.

   ```
   cd /your/download/directory
   ./install-tl
   ```

4. Enter command ‘i’ for installation

5. Post-Installation configuration:
   http://www.tug.org/texlive/doc/texlive-en/texlive-en.html#x1-320003.4.1

6. Set the path for the directory of TexLive binaries in your .bashrc file

For 32bit OS

For Bourne-compatible shells such as bash, and using Intel x86 GNU/Linux and a default directory setup as an example, the file to edit might be

```
edit $~/.bashrc file and add following lines
PATH=/usr/local/texlive/2011/bin/i386-linux:$PATH;
export PATH
MANPATH=/usr/local/texlive/2011/texmf/doc/man:$MANPATH;
export MANPATH
INFOPATH=/usr/local/texlive/2011/texmf/doc/info:$INFOPATH;
export INFOPATH
```

For 64bit OS

```
edit $~/.bashrc file and add following lines
PATH=/usr/local/texlive/2011/bin/x86_64-linux:$PATH;
export PATH
MANPATH=/usr/local/texlive/2011/texmf/doc/man:$MANPATH;
export MANPATH
```

```
INFOPATH=/usr/local/texlive/2011/texmf/doc/info:$INFOPATH;
export INFOPATH
```

Fedora/RedHat/CentOS:

```
sudo yum install texlive
sudo yum install psutils
```

SUSE:

```
sudo zypper install texlive
```

Debian/Ubuntu:

```
sudo apt-get install texlive texlive-latex-extra
sudo apt-get install psutils
```

Appendix B

Installing the CUED class file

LaTeX.cls files can be accessed system-wide when they are placed in the <texmf>/tex/latex directory, where <texmf> is the root directory of the user's TeXinstallation. On systems that have a local texmf tree (<texmflocal>), which may be named "texmf-local" or "localtexmf", it may be advisable to install packages in <texmflocal>, rather than <texmf> as the contents of the former, unlike that of the latter, are preserved after the LaTeXsystem is reinstalled and/or upgraded.

It is recommended that the user create a subdirectory <texmf>/tex/latex/CUED for all CUED related LaTeXclass and package files. On some LaTeXsystems, the directory look-up tables will need to be refreshed after making additions or deletions to the system files. For TeXLive systems this is accomplished via executing "texhash" as root. MIKTeXusers can run "initexmf -u" to accomplish the same thing.

Users not willing or able to install the files system-wide can install them in their personal directories, but will then have to provide the path (full or relative) in addition to the filename when referring to them in LaTeX.